International Journal of GEOMATE
(Geotechnique, Construction Materials and Environment)
ISSN: 2186-2982 (P), 2186-2990 (O), Japan
Vol. 31, Issue 144, August, 2026, pp.40-50; DOI: 10.21660/2026.144.5474

FINITE ELEMENT ASSESSMENT OF W-BEAM ON INDONESIAN HIGHWAY ALIGNMENTS

*Siti Rahma[1], Rudy Hermawan Karsaman[1], Aine Kusumawati[1,] and Mahesa Akbar[2]

[1] Department of Civil Engineering, Faculty of Civil and Environmental Engineering, Bandung Institute of Technology, Indonesia, [2] Department of Aerospace Engineering, Faculty of Mechanical and Aerospace Engineering, Bandung Institute of Technology, Indonesia

*Corresponding Author, Received: 06 Feb. 2026, Revised: 26 April 2026, Accepted: 07 May 2026

ABSTRACT: Road safety is currently one of Indonesia's national programs. The program includes implementing forgiving roads on Indonesia's toll roads. Since 2020, toll roads under construction have required the use of W-beam as roadside safety barriers. As an archipelagic nation, Indonesia has diverse topography, including lowlands, mountains, and extensive maritime areas. Research on the safety performance of W-beam under various geometric scenarios in Indonesia remains limited to this day. Therefore, this study employs finite element simulations using Abaqus/Explicit to evaluate the structural performance of W-beam guardrails under three representative Indonesian road alignment conditions: flat straight road, 5% downhill slope, and a 130-meter radius horizontal curve with 8% superelevation. Passenger vehicle impacts are simulated at 100 km/h with impact angles of 15°, 20°, and 25°. The simulation results show that the W-beam sustains permanent deformation under all tested scenarios. Under the 130-meter radius curve alignment, the Von Mises Stress in the W-beam remained below the material's ultimate tensile strength, suggesting a structurally favorable response compared to straight and downhill alignments; however, this finding is based solely on numerical evidence and should be further validated through physical crash testing. The findings provide preliminary simulation-based guidance for the installation of W-beam guardrails on varied road geometries in Indonesia, supporting the adaptation of international road safety standards to local topographic and design conditions.

Keywords: Road safety, W-beam, Guardrails, Finite element analysis

1. INTRODUCTION

According to data from Statistics Indonesia (BPS), the Indonesian National Police Traffic Corps reported that the accident fatality rate in Indonesia in 2022 was 20%. Rollover or lane departure are the most common types of accidents on both toll roads and non-toll roads in Indonesia. Even on toll roads, the percentage of such accidents reaches 70% [1]. Therefore, the Indonesian government is currently striving to improve road safety, one of which is through the National Road Safety Program outlined in the National Road Traffic and Transportation Safety Master Plan (RUNK). One of the pillars to be realized in this program is the implementation of safe roads. To accomplish this, one practical step that can be implemented is designing forgiving roads, such as by installing roadside safety barriers [2]. The purpose of these barriers is to provide a safe roadside environment in case vehicles veer off the roadway [3]. According to the Toll Road Regulatory Agency (BPJT), the authority responsible for toll road construction in Indonesia, one of the roadside safety barriers currently in use is the steel barrier with a wave-beam (W-beam) profile. Steel barriers are one of the road safety devices designed to contain vehicles if they lose control and leave the roadway [4]. Numerous studies have been conducted on the safety performance of W-beam guardrails, both through field crash level tests and numerical simulations.

Numerical simulations to model dynamic impacts or impacts that cause structural damage can be performed using software such as LS-DYNA, ABAQUS/Explicit, RADIOSS, and PAM-CRASH [5]. The application of the finite element method (FEM) to simulate dynamic impact behavior under explicit analysis frameworks has been extensively demonstrated across engineering disciplines. Abaqus/Explicit has been employed as a validated numerical platform for evaluating dynamic tire–road interaction characteristics and ride comfort performance under transient loading conditions [6]. FEM-based structural evaluation employing equivalent static impact forces, systematic variation of geometric parameters, and stress-versus-deflection performance criteria has been demonstrated to constitute a well-established and accepted methodology in safety-driven engineering design [7]. Generally, these crash test scenarios follow international standards, such as those outlined in several National Cooperative Highway Research Program (NCHRP) reports. According to Manual for Assessing Safety Hardware (MASH), 2016 by AASHTO, crash level tests should be conducted under extreme scenarios and conditions, such as speeds and geometric. Therefore, this study will conduct numerical simulations of vehicle crash tests with W-beam based on typical road geometric conditions in Indonesia, as outlined in the Geometric Design Guidelines for Roads (PDGJ) which are applicable in Indonesia.

The safety performance of barriers is assessed based on the vehicle's behavior immediately after the impact [4]. Road safety barriers are deemed safe under certain conditions, including no rollover, no tilt exceeding 75°, and no damage to the occupant compartment. Additionally, based on Austroads' road safety conditions, the safety performance of guardrails can be evaluated based on the following factors: structural strength, vehicle and occupant risk, and prediction of the possible vehicle trajectory after impact [8]. There are four categories of vehicle movement behavior post-impact, as listed below: Redirected (R), Remained in contact (RC), Spin out (SO), and Flipped over (FO) [6]. From these four conditions, it can be concluded that the (R) and (RC) conditions can be categorized as safe, which means the risk of occupant injury is lower compared to the (SO) and (FO) conditions. The level of passenger injury resulting from accidents is described as follows:

K : fatal injury
A : incapacitating injury
B : non-incapacitating injury
C : possible injury
O : no injury [9]

The (SO) and (FO) conditions often cause secondary incidents when the vehicle re-enters the roadway [10]. However, in this redirected condition, the vehicle must still be within the exit box area with an exit angle of no more than 14° degrees. The exit angle is determined by the angle between the centerline of the vehicle and the guardrail when the vehicle moves away from the guardrail after an impact [11]. If this value is too wide, it will cause the vehicle to enter the lane too far. The likelihood of a secondary accident occurrence will decrease if the exit angle is 60% smaller than the impact angle. The impact angle is formed between the longitudinal centerline of the vehicle and the longitudinal axis of the guardrails at the time of the impact [12]. If the initial impact angle is 20°, the exit angle must not exceed 12°. The following is an illustration of the vehicle's position and the guardrail during the impact.

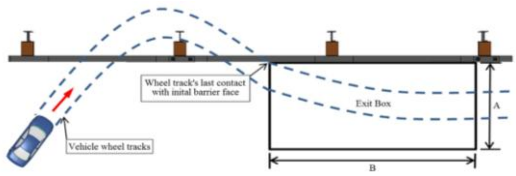

Fig. 1 Illustration of a vehicle impact [11]

The safe exit box dimensions according to MASH, 2016 are presented in Table 1 below.

Table 1. Specifications of exit box [4]

Vehicle type	Dimension of Exit Box	
	A	B
Passenger car/truck/pick-up	$\mathbf{7.2} + \boldsymbol{V_w} + \mathbf{0.16}\boldsymbol{V_L}$ (ft)	32.8 ft (10.0 m)
1996 Dodge Neon	15.1 ft (4.6 m)	32.8 ft (10.0 m)
2006 Ford F250	16.9 ft (5.15 m)	32.8 ft (10.0 m)

Each type of road safety barrier has a different level of resistance [13]. Vehicles can pass through barriers in three ways, namely underriding, overriding, and penetration [14]. Penetration occurs when the barrier structure was not strong enough to withstand the impact force caused by a vehicle impact. Additionally, it is recognized that safety barriers with inadequate height dimensions can also cause this condition [15]. In steel barriers, the initial contact point of the impact between the vehicle and the barrier can also determine the final position of the vehicle. If a vehicle collides with the guardrail at a point between two posts, there is no contact between the tires and the posts, so the vehicle will slide along the guardrail. However, if the vehicle collides with a post, direct contact between the vehicle's wheels and the post will cause a shock, causing the vehicle to tend to penetrate the guardrail and exit the roadway [16].

W-beam is one of the steel barrier profiles and is classified as a flexible type [8]. It is referred to as a semi-flexible barrier because it can deform significantly upon impact with a vehicle and often experiences displacement as a result of the impact energy. During an impact, W-beam plays a crucial role in reducing vehicle speed, preventing vehicles from leaving the lane, and significantly reducing the likelihood of secondary accidents [17]. Therefore, this road barrier is considered safer for occupants compared to concrete barriers [18]. Additionally, W-beams do not require expensive maintenance costs and have an attractive appearance, making them widely used in various countries. Maintenance of steel barriers is conducted every three years for interstate highways and every five years for non-interstate highways [19]. W-beams are commonly found on road curves, but impacts between motorcyclists and W-beam guardrails at those locations often result in fatalities [20].

Several categories of roadside safety barriers are in current use internationally, including flexible W-beam (wave-beam) guardrails, semi-rigid thrie-beam barriers, cable median barriers, and rigid concrete barriers such as the New Jersey profile and F-shape barrier. Each system offers distinct trade-offs in terms of structural stiffness, energy absorption, deflection capacity, installation cost, and maintenance requirements. Rigid concrete barriers provide high containment capacity but transfer greater forces to occupants and are associated with higher injury severity in oblique impacts [11]. Cable median barriers are highly effective for low-angle median crossovers but are unsuitable for locations requiring minimal deflection or where roadside clearance is limited [12]. Thrie-beam barriers offer improved vehicle capture relative to W-beam, particularly for taller vehicles, but require more material and greater installation depth [4]. In contrast, W-beam guardrails remain the most widely deployed flexible barrier system globally due to their cost-effectiveness, ease of fabrication, and capacity to absorb kinetic energy through controlled deformation [15][16]. While their performance under standard flat-terrain crash test conditions is well documented through physical crash testing programs such as NCHRP Report 350 and MASH 2016, their structural response under terrain-specific conditions representative of developing nations with complex topography—such as Indonesia—remains insufficiently explored. Numerical studies have examined W-beam performance on sloped medians [8], optimised cross-section geometry [9], and compared alternative guardrail materials [10][15]; however, the combined influence of downhill gradient and horizontal curvature on the impact mechanics of W-beam under Indonesian geometric design standards has not been previously reported. The applicability of these findings to other countries will depend on regional factors including local design standards, vehicle fleet characteristics, road surface conditions, and climatic influences; such considerations are discussed in the context of the results.

The present study addresses this gap by conducting finite element simulations of passenger vehicle impacts on W-beam guardrails installed under three road alignment scenarios representative of Indonesian highway design: a flat straight road, a 5% downhill gradient, and a 130-meter radius horizontal curve with 8% superelevation. The study aims primarily to demonstrate the feasibility of Abaqus/Explicit modelling for these alignment scenarios and to generate preliminary simulation-based evidence on the structural behavior of the W-beam under local geometric conditions, in support of adapting international road safety standards to Indonesian practice. The parameters adopted follow the MASH, 2016 framework, thereby ensuring relevance to established crash testing practice.

2. RESEARCH SIGNIFICANCE

This study aims to measure the safety performance of w-beam, which are commonly used as roadside barrier on highways. This research is important because there is a limited research on vehicle response to such crash tests and it is beneficial to have better understanding on the structural strength of steel barrier when installed in geometric road scenarios in Indonesia. The parameters used in this study are based on the MASH, 2016; thereby strengthening the relevance of findings to established crash testing practice and supporting the adjustment of international road safety standards to Indonesian conditions.

3. METHODS

This study uses a numerical simulation approach based FEM to analyze the dynamic response of passenger vehicles when colliding with road safety barriers. FEM is a numerical method used to solve continuous mechanics problems by discretizing the structural domain into a number of interconnected finite elements. With the development of computer technology, computer-based FEM solutions enable the completion of technical engineering that previously could not be solved efficiently [21]. This study uses Abaqus CAE software to measure the structural performance of W-beam steel guardrails. The simulation is carried out by implementing a composite material model to identify the elasticity, failure, and post-failure properties of the research object. In addition to W-beams, passenger cars are also the subject of this study. There are three pillars that must be defined in the Finite Element Method, namely:

- Physical phenomena
- Discretization
- Interpolation [22]

In this study, the interpolation function is not formulated explicitly, but is integrated into the

Abaqus element formula. The form and order of interpolation are determined by the selection of elements, the number of nodes, and the mesh setting strategy.

3.1 Geometric Design of Research Objects

The physical phenomena in Abaqus CAE were implied by drawing the geometry and determining the physical contact between the two research objects. Based on NCHRP Report 350, the selection of the planned vehicle type was carried out using vehicles commonly used by road users. To represent these conditions, this study used passenger cars as the planned vehicles. The passenger car to be simulated in this simulation has a vehicle weight of 1,000 kg, with a height of 1,485 mm, a width of 1,680 mm, and a length of 3,795 mm. The vehicle was modelled as a deformable shell structure using four-node shell elements (S4R), which is a simplified but widely employed surrogate model in guardrail FEM studies [8][15]. This approach captures the primary deformation mechanics of the vehicle body without the computational cost of a full vehicle model. The total mass of 1,000 kg was distributed uniformly across the shell components, with the material properties of AISI 1010/SPCC cold-rolled steel applied as described in Section 3.2. While the model does not include interior substructure, engine block, or suspension, these simplifications are consistent with the NCHRP Report 350 test level TL-3 surrogate vehicle approach and are appropriate for evaluating guardrail structural response rather than detailed occupant injury prediction.

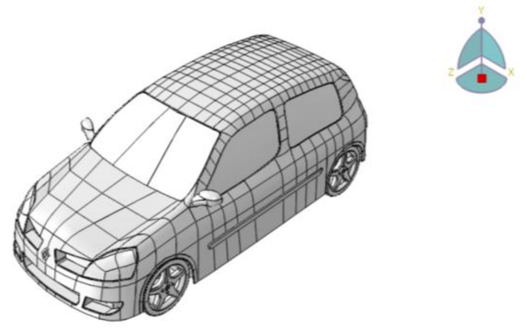

Fig. 2 FEM of the passenger car

The steel barrier used in this study is the W-beam type, a double-curved beam plate safety barrier that meets the technical specifications applicable in Indonesia [23]. The dimensions of the FEM model of this W-beam barrier are 20 meters long. The cross section of w-beam is shown in Figure 3.

3.2 Material Specifications of Research Objects

The steel barrier material must comply with the requirements of JIS G 3101 (ASTM A36/A36M-19) for general rolled steel structures [24]. Steel safety barriers must also be securely installed. Therefore, in this model, the steel posts are made rigid or immovable. Each post in the steel safety barrier must be anchored to or founded on a minimum depth of 100 cm The W-beam posts used in this model are standard C-channel steel sections (C150×75 mm) with a wall thickness of 9 mm, consistent with Indonesian Ministry of Transportation specifications [21]. The posts are connected to the W-beam rail via spacer blocks, and the bolt connections are represented by tie constraints between the spacer and rail contact surfaces. The decision to treat the posts as fully rigid (encastre boundary condition at the base) constitutes a simplifying assumption that maximizes the stiffness of the system and may result in an underestimation of energy dissipation during impact. In practice, post yielding and soil-post interaction contribute to the overall energy absorption of the guardrail system [8]. This assumption is therefore conservative with respect to W-beam stress predictions and should be addressed in future work through sensitivity analyses incorporating soil-spring boundary conditions or deformable post models. [23]. The material properties will be input into the properties of the numerical simulation object, while the description of the steel safety barrier material can be seen in Table 2.

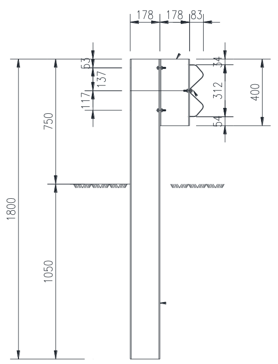

Fig. 3 Cross-sectional view of a W-beam

Table 2. Specifications of steel barrier material

No	*Properties*	*Values*
1	Density	7,850 kg/m3
2	Yield strength	245 MPa
3	Ultimate tensile strength	500 MPa
4	Modulus Elasticity	200,000 Mpa

The Table 3 following is the input data at the description stage of the steel barrier material properties:

Table 3. W-beam material properties input data (JIS G3101)

Elastic	
Young Modulus	*Poisson's Ratio*
200000	0.3
Plastic	
Plastic Yield Stress	*Plastic Strain*
245	0
300	0.05
400	0.15
500	0.3

In addition to steel barrier materials, this material input is also used in light passenger vehicles. In the Table 4 is the AISI 1010/SPCC material input.

Table 4. AISI 1010/SPCC as vehicle material properties input data

Elastic	
Young Modulus	*Poisson's Ratio*
200,000	0.3
Plastic	
Plastic Yield Stress	*Plastic Strain*
300	0
350	0.05
400	0.15

The simulation in this study was designed in accordance with the field crash test philosophy contained in NCHRP Report 350. The validity of the test was determined by the suitability of physical parameters, namely vehicle type, speed, and impact angle. The success of the safety barrier structure in absorbing collision energy was a determining factor in the acceptance of the crash test. Therefore, the conclusions of this simulation are not drawn from statistical repetition but use a deterministic exploratory approach with a focus on a number of technically selected critical scenarios. The selected road geometry scenarios are as follows: Material failure in the W-beam was modelled using the ductile damage initiation criterion available in Abaqus/Explicit, with element deletion activated when the equivalent plastic strain at a given integration point reaches the fracture strain defined by the plastic hardening curve (Table 3). This approach corresponds to progressive element erosion, which removes elements that have exceeded their failure criterion and thereby prevents artificial stress lock-up. Strain-rate effects were not explicitly incorporated in the current model through a Johnson–Cook viscoplastic formulation; this is acknowledged as a limitation, given that high-rate impacts at 100 km/h can increase the apparent yield stress of structural steel by 10–30% relative to quasi-static values. The influence of this simplification on the reported stress magnitudes should be considered when interpreting results. Contact between the vehicle and the W-beam guardrail was defined using the Abaqus/Explicit general contact algorithm with a penalty-based enforcement method. A coefficient of friction of 0.3 was assigned to all steel-to-steel contact pairs, consistent with values reported in comparable W-beam FEM studies [8][15]. Contact stabilization was applied to prevent initial geometric penetration at the start of the simulation. The contact formulation captures both normal pressure and tangential frictional forces, which are critical for accurately representing the vehicle sliding behavior along the guardrail after initial impact.

- The road slope used a 5% gradient, which is the maximum gradient specified for highways on flat terrain [25].
- The curved road scenario was conducted by determining the selected design speed for inter-city roads, type 2/2 undivided, which is 50 km/h. With this design speed, the selected curve radius is 130 meters with an 8% superelevation [25].

According to MASH, 2016; the impact angles are 15°, 20°, and 25°. In the Abaqus modeling, the angle difference is facilitated by the position of the vehicle and guardrail relative to the global axes (X, Y, Z). In addition, there are several conditions to minimize directional bias in this simulation, namely:

- The passenger car collided directly with the W-beam post.
- The moment of initial contact between the car and the W-beam occurred at a height of 200 mm from the round surface.

In Abaqus input, force vectors are not adjustable. Therefore, in the scenario of a 5% slope road with a 130-meter radius curve, the position of the assembly in terms of elevation and the placement of the two research objects must be adjusted. The following are the images of Computer Aided Design (CAD) assembly model in both conditions.

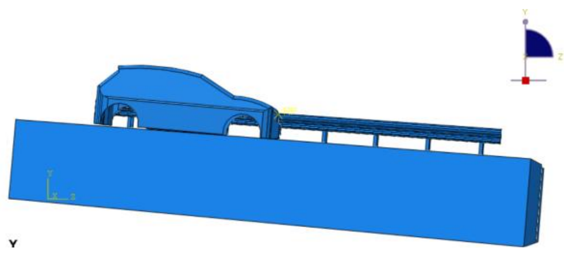

Fig. 4 CAE Assembly in a 5% slope descent

In the data input, the definition of vehicle velocity direction used is Translation, which refers to the displacement or straight movement of the vehicle from one location to another. The velocity taken is the maximum impact velocity according to the crash level test specifications [4]. In this modeling, the velocity unit input is adjusted to the unit used when drawing the safety barrier geometry, which is mm/s. On the (Z) axis, the velocity given to the vehicle is as follows:
Vehicle speed (V) = 27.777,8 mm/s.

3.3 Discretization

Discretization is the process of dividing a domain into smaller subdomains. A subdomain is a section bounded by lines connecting nodes. The more nodes analyzed, the more accurate the values or data will be. To support the discretization step in this simulation, each research object is described as a solid tetrahedron element. This element has four nodes, and each node has 3 displacements in each direction: x, y, and z. In Abaqus CAE modeling, this discretization is done by determining the mesh size. In the Mesh module, both the vehicle and the w-beam are described as tetrahedral elements with sizes of 50 for the car, 100 for the upper part of the w-beam structure, and 150 for the w-beam posts. This measurement is also used to calculate the surface area affected by the impact. The time used for crash simulation under certain geometric conditions is greater than or equal to 5 seconds The mesh sizes quoted above are in millimeters (mm): 50 mm for the vehicle body panels, 100 mm for the W-beam rail, and 150 mm for the post elements. The element type used is the four-node linear tetrahedron (C3D4). To evaluate the sensitivity of the results to mesh density, a preliminary check was performed by comparing peak von Mises stress in the W-beam rail for the flat-road, 20°-impact scenario using the baseline mesh (100 mm) and a finer mesh (50 mm). The peak stress values differed by less than 5%, indicating that the selected mesh sizes provide a sufficiently converged solution for the stress and damage-area metrics reported in this study. Regarding impact angle implementation, the angle between the vehicle's velocity vector and the longitudinal axis of the guardrail was established by rotating the vehicle assembly about the global vertical axis (Z-axis), while the guardrail remained aligned with the global X-axis. The initial velocity was applied as a translational body force in the direction of the vehicle's heading, with the magnitude resolved into components normal and tangential to the guardrail. For the 5% downhill slope scenario, the slope was modelled by rotating the entire assembly (vehicle and guardrail) about the transverse axis, and gravity was applied as a body force in the global vertical direction. The 130-meter radius curve scenario was implemented by positioning the guardrail along the curved path and orienting the vehicle tangentially to the curvature at the initial contact point, with superelevation of 8% applied as a cross-slope to the assembly. The 5-second simulation duration was selected based on the requirement specified in NCHRP Report 350 [4] and is sufficient to capture the full vehicle engagement with the guardrail, the post-impact redirection phase, and the subsequent free trajectory of the vehicle away from the barrier [4]. Therefore, the results of this crash test simulation will observe the stress values that occur during the 5-second observation period.

4. RESULTS AND ANALYSIS

In the Table 5 below shows the summary of the w-beam and passenger car stress values. In addition, in the Figure 4 shows the simulation results with the highest stress values experienced by the vehicle and w-beam in a road geometry scenario with a 5% slope and a 20° impact angle.

In the following equations are the examples of the calculation to determine the extent of damage to the w-beam and passenger car or vehicle.

Damage area of the W-beam
= 4,400 x 300 = 1,320,000 mm^2

Damage area of the passenger vehicle
= 550 x 717 = 394,350 mm^2

From the simulation results, during the 5-second observation period, the stresses experienced by the W-beam exceeded the ultimate tensile strength limit of the material properties, which is 500 MPa, at every impact speed and angle in all road geometry scenarios. At the same impact speed, the stresses experienced by the W-beam tend to increase in line with the increase in the impact angle. According to elasticity theory, if the stress exceeds the maximum tensile strength limit, the material will fracture. The simulation results show that the stress on the W-beam at the 5-second observation point in the 130-meter radius curve geometry scenario is lower than in the other two geometry scenarios. The stress on the W-beam in the 130-meter radius curve has exceeded the yield strength limit of 245 MPa but is still below the ultimate tensile strength limit of 500 MPa. Once the stress exceeds the yield strength, the material enters the plastic zone, where it undergoes permanent deformation.

Table 5. Stress values on the W-beam and the passenger car

No	Road type alignment	Speed (km/h)	Impact angle (°)	Stress (MPa)			
				W-beam	Maximum tensile strength limit of w-beam	Passenger car	Maximum tensile strength limit of passenger car
1	Straight and flat	100	15	518	500	428	400
			20	567		381	
			25	577		311	
2	5% downhill slope	100	15	532		332	
			20	687		422	
			25	584		307	
3	130 m radius curve	100	15	403		456	
			20	460		461	
			25	483		456	

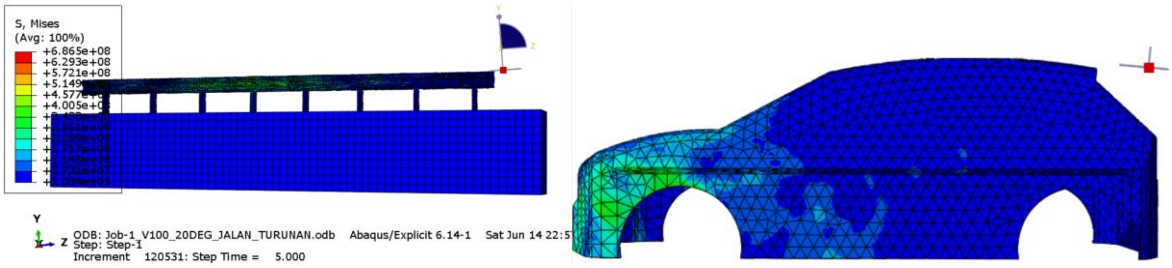

Fig. 5 Damage to the W-beam and the passenger car on a road with 5% downhill slope

Table 6. Summary of the damage areas of the W-beam and the passenger car for each scenario

No	Road type alignment	Speed (km/h)	Impact angle (°)	Damage area (mm^2)		Post-impact vehicle position
				W-beam	Passenger car	
1	Straight and flat	100	15	394,350	1,320,000	Redirected
			20	537,750	1,320,000	Redirected
			25	752,850	1,155,000	Redirected
2	5% downhill slope	100	15	394,350	990,000	Redirected
			20	537,750	990,000	Redirected
			25	752,850	1,320,000	Redirected
3	130 m radius curve	100	15	752,850	1,650,000	Redirected
			20	752,850	1,485,000	Redirected
			25	752,850	1,320,000	Redirected

In the straight road scenarios with impact angles of 15° and 20°, and the downhill road scenarios with impact angles of 15° and 25°, the vehicle has exceeded the yield strength of the vehicle's material properties, which is 300 MPa, but remains below the ultimate tensile strength of 400 MPa. From these values, it can be concluded that the passenger vehicle experiences deformation and structural changes, or is in a state of minor damage. For the other scenarios, the vehicle has exceeded the ultimate tensile strength of its material properties, meaning the vehicle suffers significant damage at certain points.

From the stress distribution diagram experienced by the W-beam and the passenger vehicle, the maximum stress occurs at the first point of contact due to the impact of the passenger vehicle. The extent of damage to the W-beam increases with the increase in the collision angle in each road geometry scenario. Only on the 130-meter radius curve does the extent of damage have the same value for each collision angle. Additionally, the damage to the passenger vehicle is predominantly observed on the side of the vehicle, with the damage area having nearly the same value across all geometric scenarios. On a 5% slope road geometry, as the collision angle increases, the damage area of the passenger vehicle also increases. This differs from the flat straight road and 130-meter radius curve scenarios, where the damage to the passenger vehicle decreases slightly as the collision angle increases. It is important to note that in Abaqus/Explicit simulations, peak von Mises stress values reported at a single time step may be influenced by dynamic wave effects and stress concentrations at mesh boundaries, particularly at element deletion sites. The reported stress values exceeding 500 MPa in Table 5 should therefore be interpreted as indicative of material fracture at localized zones rather than as uniformly distributed failure across the guardrail cross-section. The progressive accumulation of element deletion at the first contact zone is consistent with the physical mechanism of localized tearing observed in full-scale crash tests with W-beam guardrails [24]. The reported damage areas (Table 6) provide a complementary metric that is less sensitive to localized stress spikes and better reflects the overall extent of structural engagement. The lower W-beam stress observed in the 130-meter radius curve scenario relative to the straight and downhill alignments can be attributed to the reduction in the velocity component acting normal to the guardrail face. On a horizontally curved alignment with 8% superelevation, the vehicle approaches the guardrail at an effective impact angle that incorporates a lateral component induced by the centripetal tendency of the vehicle. The superelevation tilts the road surface such that the vehicle's weight vector has a component directed toward the road center, partially counteracting the lateral momentum driving the vehicle into the barrier. Consequently, the normal impact force—which governs W-beam bending and stress—is reduced relative to an equivalent straight-road impact at the same nominal impact angle and speed. This kinematic argument is consistent with findings from previous studies on guardrail performance on sloped and curved alignments [8]. The uniform damage area across impact angles in the curve scenario (Table 6) further supports this interpretation, as the reduced normal force limits the spatial spread of plastic deformation regardless of the nominal angle. In all nine simulation scenarios, the vehicle was redirected (R condition per Austroads classification [6]), indicating that the W-beam successfully contained the vehicle and prevented lane re-entry at an uncontrolled trajectory. The exit angles in all scenarios were visually assessed from the animation output to be within the safe exit box dimensions specified by MASH 2016 (Table 1), with the vehicle departing the guardrail at angles estimated to be less than 60% of the respective impact angles. Residual velocities were not quantitatively extracted in this study, which is acknowledged as a limitation; future work should include explicit extraction of exit angle and residual velocity from simulation output to enable a more rigorous assessment of occupant risk indices such as the Acceleration Severity Index (ASI) and Occupant Impact Velocity (OIV). Regarding the sensitivity to impact location (mid-span versus post-hit), this study simulated direct post-hit impacts in all scenarios (vehicle centered on a post at first contact). As discussed in the Introduction, post-hit impacts represent the more critical condition for vehicle penetration risk, and the results therefore provide a conservative estimate of W-beam structural demand. The applicability of these findings to road safety practice in other countries requires consideration of regional factors. The geometric design parameters (gradient limits, curve radii, superelevation rates) used in this study are governed by Indonesian road design guidelines (PDGJ) [23], which are broadly consistent with AASHTO Green Book standards but differ in certain threshold values. The vehicle model (1,000 kg passenger car) is representative of the predominant vehicle class in the Indonesian fleet and corresponds to the MASH TL-3 test vehicle category. Countries with significantly different vehicle fleet compositions (e.g., higher proportions of sport utility vehicles or heavier passenger cars) may exhibit different interaction kinematics with W-beam guardrails. Furthermore, scale effects arising from differences in the absolute dimensions of W-beam profiles (cross-section depth, rail thickness) between national standards should be considered when comparing simulation results across jurisdictions. The numerical results reported here are directly applicable to the specific W-beam profile conforming to Indonesian Ministry of Transportation specifications [21] and should not be generalized without appropriate modification of model geometry and material parameters.

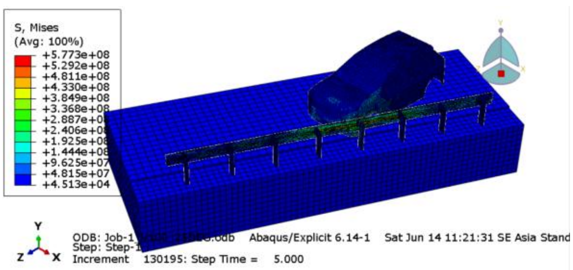

Fig. 6 Final position of the passenger car after impact in flat straight road scenario

In addition to the stress values indicated by the Abaqus CAE simulation output, the Abaqus CAE simulation can generate animations showing the vehicle's movement during the crash test observation period. From Table 6 above, during the 5-second observation period, the vehicle continues to slide along the W-beam or be in a redirected position. In the Figure 6 until Figure 8 are the final positions of the vehicles at a 25° impact angle in each road geometry scenario.

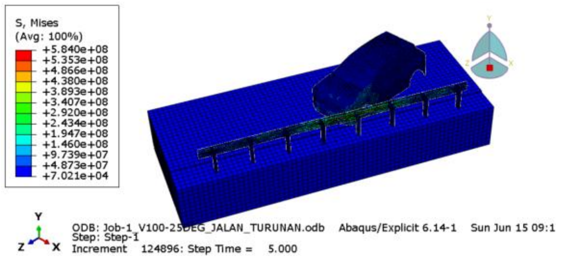

Fig. 7 Final position of the passenger car after impact in a 5% downhill scenario

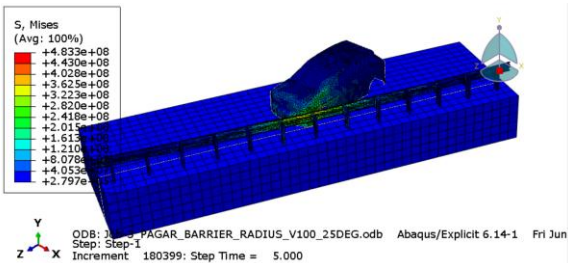

Fig. 8 Final position of the passenger car after impact in a 130-meter radius curve scenario

The simulation results of the passenger vehicle crash test with a steel guardrail in this study will also be based on the field crash test described in NCHRP Report 115 on Guardrail Performance and Design. The field crash test was conducted using a 1963 Plymouth light vehicle weighing 4,051 lb or 1,837 kg, at a speed of 60.1 mph or 96.7 km/h with an impact angle of 27.80°. The steel guardrail used was the New York W-beam type with a height of 76.2 cm above ground level. The following is a photo of the results of the field crash test.

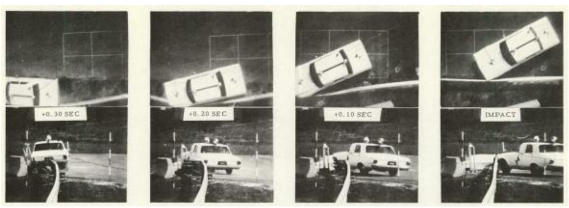

Fig. 9 Crash level test involving a passenger vehicle and W-beam [26]

From the Figure 9, it is shown that at +0.30 seconds after the impact, the vehicle is still located or moving along the steel guardrail. This is consistent with the simulation results for each geometric road scenario discussed earlier. The steel guardrail undergoes deformation or bending at the first point of contact between the vehicle and the guardrail. Therefore, it can be concluded that the results of the numerical simulations conducted on the W-beam are similar to the field crash test results reported in NCHRP 115 [26]. From previous studies, it is known that steel barriers will absorb moderate impact energy, because the impact energy is also absorbed by the colliding vehicle [13][17]. This condition is evident from the deformation of the W-beam and the increased vehicle stress during the simulation period. Additionally, the impact of a collision with a steel barrier will reduce the vehicle's speed and prevent the vehicle from leaving the road.

5. CONCLUSION

W-beam barriers are designed to absorb collision energy, but they are not intended for high speeds such as 100 km/h. Collisions at this speed on a straight, flat road, a 5% downhill slope, and a curve with a radius of 130 meters will result in permanent deformation of both the W-beam and the passenger car. There are no significant differences in stress values across the various road type alignment and impact angle scenarios. The damage sustained by the W-beam and the passenger vehicle also shows that there are no significant differences. However, as the impact angle increases, the extent of damage to both the W-beam and the passenger vehicle becomes greater. The W-beam located on a 130-meter radius curve did not fracture because of the 100 km/h impact speed with various impact angles. From this structural response, it can be indicated that the W-beam is a suitable roadside safety barrier system to be installed in this road type alignment. This research involves numerical simulations, so further field crash level testing is still required for subsequent studies. The lower stress levels recorded in the 130-meter radius curve scenario, relative to the flat and downhill alignments, are attributed to the reduction in the normal impact velocity component arising from the combined effects of horizontal curvature and superelevation, which partially counteracts the lateral momentum of the vehicle. This finding provides preliminary simulation-based evidence that W-beam guardrails may exhibit more favorable structural performance on curved road sections than on straight downhill alignments, and this observation warrants further investigation through physical crash tests and more detailed numerical models incorporating deformable posts and soil–structure interaction. The key contributions of this study are as follows: (1) it establishes a reproducible Abaqus/Explicit modelling framework for W-beam guardrail performance evaluation under Indonesian road geometry conditions; (2) it generates a set of benchmark stress and damage-area results for three alignment scenarios and three impact angles at MASH TL-3 speed; and (3) it identifies the 130-meter radius curve with 8% superelevation as a geometrically favorable condition for W-beam installation from a structural performance perspective. From a practical standpoint, the results support the continued use of W-beam guardrails on Indonesian toll roads with varied topography, particularly on curved sections, while emphasizing the need for regular maintenance given the confirmed occurrence of permanent deformation at high-speed impacts. Limitations of this study include the use of a simplified vehicle model, the absence of post-yielding soil behavior, the omission of strain-rate effects, and the qualitative nature of the validation. Future research should address these limitations through full-scale physical crash testing conducted in accordance with MASH 2016 requirements, and should include occupant risk metric evaluation (ASI, OIV) to provide a more comprehensive assessment of safety barrier performance under Indonesian road conditions.

6. ACKNOWLEDGMENTS

This research was supported by funds from the Indonesian Education Scholarship Program (BPI), the Center for Higher Education Funding and Assessment (PPAPT) under the Ministry of Higher Education, Science, and Technology of the Republic of Indonesia, and the Indonesia Endowment Fund for Education Agency (LPDP) awarded to Siti Rahma (grant number: 202101121693).

7. REFERENCES

1. Ministry of Public Works and Housing of the Republic of Indonesia and Directorate General of Highways, Technical Guideline 1: Road Safety Engineering. Jakarta: Directorate General of Highways, 2012, pp. 1-120.
2. Austroads, Guide to Road Design Part 6: Roadside Design, Safety and Barriers. Edition 4.0, Sydney: Austroads, Ltd. 2024, pp. 1-264. ISBN: 978-1-922994-44-8.
3. Gabauer, D. J. and Gabler, H. C., Comparison of Roadside Crash Injury Metrics Using Event Data Recorders. Accident Analysis and Prevention, Vol. 40, No. 2, 2008, pp. 548–558. https://doi.org/10.1016/j.aap.2007.08.011
4. American Association of State Highway and Transportation Officials, Manual for Assessing Safety Hardware. AASHTO, United States of America, 2nd Edition, 2016, pp. 1-274. ISBN: 978-1-56051-665-1.
5. Wade, B., Feraboli, P., Osborne, M., and Rassaian, M., Simulating Laminated Composite Materials Using LS-DYNA Material Model MAT54: Single-Element Investigation. Final Report No DOT/FAA/TC-14/19. U.S. Department of Transportation, Federal Aviation Administration, 2015, pp. 1-63. https://www.researchgate.net/publication/322152587
6. Suvanjumrat C. and Rugsaj R., The Dynamic Finite Element Model of Non-Pneumatic Tire Under Comfortable Riding Evaluation, International Journal of GEOMATE, Vol. 19, Issue 76, 2020, pp. 62–68. https://doi.org/10.21660/2020.76.9135
7. Wongchai B., Front and Side Impact Analysis of Space Frame Chassis of Formula Car, International Journal of GEOMATE, Vol. 18, Issue 67, 2020, pp. 168–174. https://doi.org/10.21660/2020.67.5528
8. Austroads, Guide to Road Safety Part 2: Safe Roads. Edition 1.0, Sydney: Austroads Ltd, 2021, pp. 1-242. ISBN: 978-1-922382-60-3.
9. Russo, B. J. and Savolainen, P. T., A Comparison of Freeway Median Crash Frequency, Severity, and Barrier Strike Outcomes by Median Barrier Type. Accident Analysis Prevention, Vol. 117, 2018, pp. 216–224. https://doi.org/10.1016/j.aap.2018.04.023
10. Gutowski, M., Palta, E., and Fang, H., Crash Analysis and Evaluation of Vehicular Impacts on W-Beam Guardrails Placed on Sloped Medians Using Finite Element Simulations. Advances in Engineering Software, Vol. 112, 2017, pp. 88–100. http://dx.doi.org/10.1016/j.advengsoft.2017.04.004
11. Hou, S., Tan, W., Zheng, Y., Han, X., and Li, Q., Optimization Design of Corrugated Beam Guardrail Based on RBF-MQ Surrogate Model And Collision Safety Consideration. Advances in Engineering Software, Vol. 78, 2014, pp. 28–40. http://dx.doi.org/10.1016/j.advengsoft.2014.08.002
12. D Sun, S., Li, H., Zhu, C., Mei, K., Jiang, H., Sun, Y., and Huang, H., Study on The Anti-Collision Performance of Basalt Fiber Reinforced Polymer Beam–Column Guardrail. Composite Structures,

Vol. 276, 2021, pp. 1-12. https://doi.org/10.1016/j.compstruct.2021.114588

13. Butans, Ž., Gross, K. A., Gridnevs, A., and Karzubova, E., Road Safety Barriers, the Need and Influence on Road Traffic Accidents. IOP Conference Series: Materials Science and Engineering, Vol. 96, 2015. https://iopscience.iop.org/article/10.1088/1757-899X/96/1/012063
14. Alluri, P., Gan, A., Haleem, K., and Mauthner, J., Safety Performance of G4 (1S) W-Beam Guardrails versus Cable Median Barriers on Florida's Freeways. Journal of Transportation Safety and Security, Vol. 7, No. 3, 2015, pp. 208–227. http://dx.doi.org/10.1080/19439962.2014.947394
15. Molan, A. M., Moomen, M., and Ksaibati, K., The Impact Of Traffic Barrier Geometric Features on Crash Frequency and Injury Severity of Non-Interstate Highways," Journal of Safety Research, Vol. 75, 2020, pp. 155–165. https://doi.org/10.1016/j.jsr.2020.09.005
16. Jiga, G., Stamin S., Popovici, D., and Dinu, G., Study of Shock Attenuation for Impacted Safety Barriers. Procedia Engineering, Vol. 69, 2014, pp. 1191–1200. https://doi.org/10.1016/j.proeng.2014.03.109
17. Wang, L., Huang, X., Li, R., Tang, Z., Li, J., and Chen, D., Collision Study on New Aluminum Alloy W-Beam Guardrail. Applied Sciences, Vol. 14, No. 12, 2024, pp. 1-16. https://doi.org/10.3390/app14125266
18. Neves, R. R., Fransplass, H., Langseth, M., Driemeier, L., and Alves, M., Performance of Some Basic Types of Road Barriers Subjected to the Collision of A Light Vehicle. Journal of the Brazilian Society of Mechanical Sciences and Engineering, Vol. 40, No. 6, 2018, pp. 1-14. https://doi.org/10.1007/s40430-018-1201-x
19. Alluri, P., Kirolos, H., and Gan, A., In-Service Performance Evaluation (ISPE) for G4 (1S) Type of Strong-Post W-Beam Guardrail System and Cable Median Barrier: Volume I. Final Report Contract No. BDK80977-I9, Lehman Center For Transportation Research, Florida International University, 2012, pp. 1-68.
20. Jama, H. H., Grzebieta, R. H., Friswell, R., and McIntosh, A. S., Characteristics of Fatal Motorcycle Crashes into Roadside Safety Barriers in Australia and New Zealand. Accident Analysis and Prevention, Vol. 43, No. 3, 2011, pp. 652–660. https://doi.org/10.1016/j.aap.2010.10.008
21. Khennane, A., Introduction to Finite Element Analysis Using MATLAB and Abaqus, 1st Edition. Boca Raton: CRC Press, 2013, pp. 1-487. https://doi.org/10.1201/b15042
22. Young, T. Y., Finite Element Structural Analysis. Englewood Cliffs, New Jersey: Prentice Hall, Inc., 1986, pp. 1-543, ISBN-10: 0133171167.
23. Ministry of Transportation of the Republic of Indonesia, Regulation of the Minister of Transportation of the Republic of Indonesia Number PM 14 of 2021, Jakarta, 2021, pp. 1-90.
24. Ministry of Public Works and Housing of the Republic of Indonesia and Directorate General of Highways, General Specifications for Expressways and Toll Roads, Jakarta: Directorate General of Highways, 2020, pp. 1-576.
25. Ministry of Public Works and Housing of the Republic of Indonesia and Directorate General of Highways, Road Geometric Design Guidelines. Jakarta: Directorate General of Highways, 2021, pp. 1-329.
26. Highway Research Board, National Cooperative Highway Research Program (NCHRP) Report 115 Guardrail Performance and Design. National Research Council, National Academy of Sciences-National Academy of Engineering, Washington, D.C., 1971, pp. 1-66. ISBN: 0-309-01905-2.Author H., A Book New York Publisher, Year, pp.1-200.